International Journal of Pharmaceutics: X 6 (2023) 100205

Contents lists available at ScienceDirect

International Journal of Pharmaceutics: X

journal homepage: www.sciencedirect.com/journal/international-journal-of-pharmaceutics-x

Enhanced stability and skin permeation of ibuprofen-loaded solid lipid nanoparticles based binary solid lipid matrix: Effect of surfactant and lipid compositions

Thitirat Chantaburanan, Veerawat Teeranachaideekul, Anchalee Jintapattanakit, Doungdaw Chantasart, Varaporn Buraphacheep Junyaprasert *

Department of Pharmacy, Faculty of Pharmacy, Mahidol University, Sri-Ayutthaya Road, Rajathevee, Bangkok 10400, Thailand

ARTICLE INFO

Keywords:
Solid lipid nanoparticles
Binary lipid matrix
Long-term stability
In vitro drug release
In vitro skin permeation
Crystallinity, Ibuprofen

ABSTRACT

Hypothesis: The type of emulsifier selected has an impact on the physicochemical properties of solid lipid nanoparticles (SLNs). This study was designed to compare the effects of emulsifiers on the physicochemical properties and *in vitro* skin performance of SLNs prepared from a binary mixture of Softisan® 378 (S378) and cetyl palmitate (CP) to those of SLNs prepared from only CP and S378.

Experiments: SLNs were prepared from CP, S378, or a binary mixture of CP and S378 (1:1 *w*/w) as the lipid phase and stabilized with Tego®Care 450 (TG450) or poloxamer 188 (P188) containing 1.0% *w*/w ibuprofen loading. The physicochemical properties including the particle size, polydispersity index (PDI), zeta potential (ZP), encapsulation efficiency (E.E.), crystallinity (%CI), and polymorphism were determined after production and after storage for 180 days under different conditions. In addition, *in vitro* drug release and permeation through human skin was studied after production and storage at room temperature for 180 days.

Finding: The particle sizes of ibuprofen-loaded SLNs (IBSLNs) stabilized with P188 (IBSLN-P188) were smaller than those of SLNs stabilized with TG450 (IBSLN-TG450) ($p < 0.05$). After 180 days, the particle sizes of the IBSLNs were slightly increased compared to those at the initial time but were <250 nm. The IBSLN-TG450 sample showed a higher %CI than IBSLN-P188 prepared with similar propotions of CP and S378, and ibuprofen crystals were observed in the IBSLN1-TG450 sample after storage at 4 °C for 180 days. Based on the result of the *in vitro* release study and the *in vitro* skin permeation test, the addition of S378 into the CP-matrix modified ibuprofen release and skin permeation both permeated ibuprofen through the epidermis and retained ibuprofen in the epidermis. In addition, the storage time affected the release and skin permeation of ibuprofen from the SLNs, which depended on the composition of the IBSLNs.

1. Introduction

Solid lipid nanoparticles (SLNs) are promising nanocarriers composed of a solid lipid core stabilized with emulsifiers. Several advantages have been reported for these nanocarriers, including effective entrapment of lipophilic drugs, stabilization of the encapsulated drugs, improvement in the oral bioavailability, enhanced skin permeation, and sustained and prolonged release (Souto et al., 2020; Zafeiri et al., 2017; Ghasemiyeh and Mohammadi-Samani, 2018). The physicochemical properties of SLNs mainly depend on the composition, *i.e.*, lipid matrix, emulsifier, encapsulated drug (Zafeiri et al., 2017; Ghasemiyeh and Mohammadi-Samani, 2018; Souto et al., 2022; Sakellari et al., 2021), and the production techniques, *i.e.*, hot or cold high-pressure homogenization, microemulsion, and solvent emulsification/evaporation techniques.

SLNs have been used extensively in a variety of skin applications, including topical (Araujo et al., 2021; Katari and Jain, 2021) and dermal (Lucia, 2017; Shahraeini et al., 2020; Essaghraoui et al., 2019) treatments. For topical applications, the SLNs are generally composed of biocompatible, nonirritating, and nontoxic lipid materials (Souto et al., 2020; Souto et al., 2022). It has been reported that SLNs improve skin penetration of encapsulated drugs *via* formation of an occlusion film after evaporation, which reduces transepidermal water loss and increases skin moisture (Souto et al., 2022; Jain et al., 2017;

* Corresponding author at: Department of Pharmacy, Faculty of Pharmacy, Mahidol University, Rajathevee, Bangkok 10400, Thailand.
E-mail address: varaporn.jun@mahidol.ac.th (V.B. Junyaprasert).

https://doi.org/10.1016/j.ijpx.2023.100205
Received 23 May 2023; Received in revised form 3 August 2023; Accepted 7 August 2023
Available online 10 August 2023

Teeranachaideekul et al., 2017). The occlusive properties of SLNs depend on the degree of crystallinity of the lipid matrix, as indicated by the percentage of crystallinity (%CI) (Teeranachaideekul et al., 2017; Wissing and Muller, 2002; Wissing et al., 2001). Nevertheless, poor drug encapsulation, drug expulsion, and physical instability may arise due to gel formation during storage, leading to burst release instead of controlled release. Such drawbacks can be caused by lipid crystallization and polymorphic transitions occuring during storage, which are generally found in SLNs prepared from highly purified waxes or triglycerides (Chutoprapat et al., 2022; Naseri et al., 2015). To overcome these limitations, nanostructured lipid carriers (NLCs) have been developed by adding oils to the lipid matrices of SLNs, which leads to imperfect structures of the solid lipid matrices that can improve drug loading, entrapment, and stability, and reduce drug leakage during storage (Chutoprapat et al., 2022; Naseri et al., 2015). According to the literature, increases in the oil contents of NLCs resulted in lower crystallinity and more crystal defects (Teeranachaideekul et al., 2008; Pornputtapitak et al., 2019; Kovacevic et al., 2011). Therefore, the amount of oil added to the NLCs should be optimized. NLCs with high oil loading exhibited deposition of the excess oil on the surface particles (Jores et al., 2004), which resulted in low crystallinity and occlusions, loss of sustained release property, low chemical stability of the encapsulated drug, and poor skin penetration. Therefore, the addition of a secondary lipid with a different chemical structure in place of the oil might lower the incidence of these problems. SLNs prepared from a binary mixture of two solid lipids have resulted in increased drug entrapment and loading levels, desired release profiles, improved stabilities, and modified the time courses for polymorphic transitions (Bunjes et al., 1996; Rawat et al., 2011; Kheradmandnia et al., 2010). In addition, it has been reported that the type of emulsifier used can affect the crystallinity of the lipid matrix and the physicochemical properties of the SLNs, *e.g.*, the mean particle size, size distribution, zeta potential, inner structure of the SLNs, release properties, and stability of the SLNs.

For dermal applications, nonionic emulsifiers are used preferentially because of their skin compatibility. The two main groups of nonionic emulsifiers that have been commonly used to stabilize SLNs are polyethylene glycol block and polyhydroxy emulsifiers. The Tego®Care 450 (TG450) emulsifier is a polyhydroxy emulsifier comprising a central hydrophilic polyglycerol 3-methylglucose ring linked with two long saturated hydrocarbon chains, while poloxamer 188 (P188), a polyethylene glycol block emulsifier, comprises hydrophobic poly(propylene oxide) linked with two hydrophilic poly(ethylene oxide) segment as shown in Fig. 1.

In our previous study, we reported that the addition of a solid complex triglyceride, Softisan® 378 (S378), into cetyl palmitate (CP) led to a less ordered structure of the CP matrix and affected the physicochemical and release properties of the SLNs (Chantaburanan et al., 2017). To our knowledge, few SLNs with a binary lipid matrix have been prepared. In particular, the effects of emulsifiers on the *in vitro* skin performance and long-term stabilities of binary lipid matrix SLNs have not been reported. It is of our interest to investigate the effects of emulsifiers on the stability and skin performance of the binary lipid matrix after long-term storage. In this study, SLNs were prepared from CP, S378, or a binary mixture of CP and S378 (1:1 *w*/w) as the lipid phase, and they were stabilized with TG450 or P188. The physicochemical properties of the IBSLNs were observed over 180 days at three different temperatures (4 °C, RT, and 40 °C) including the particle sizes, size distributions, zeta potentials, encapsulation efficiencies (%E.E.), and chemical stabilities. In addition, the *in vitro* skin performance studies were evaluated after 180 days of storage at room temperature and compared with those at the initial time.

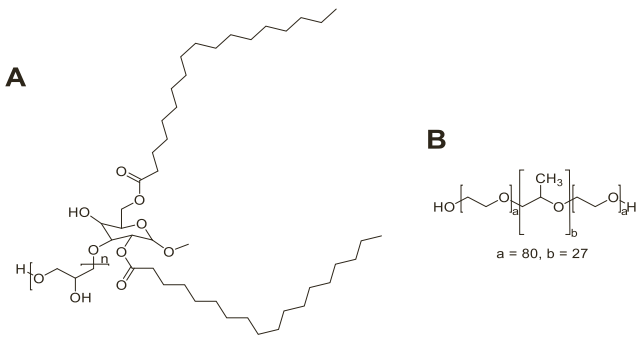

Fig. 1. Chemical structures of TG450 (A) and P188 (B).

2. Materials and methods

2.1. Materials

CP was obtained from SABO S.p.A. (Levate (BG), Italy). Softisan® 378 (S378, caprylic/capric/myristic/stearic triglycerides) and Miglyol 812 (M812, caprylic/capric triglycerides) were purchased from Sasol GmbH (Hamburg, Germany). Tego®Care 450 (TG450, polyglyceryl-3 methylglucose distearate) was gifted from Evonik Industries AG (Essen, Germany). Poloxamer 188 (P188) was gifted from BASF (Ludwigshafen, Germany). Ibuprofen was purchased from HuBei Granules-Biocause Pharmaceutical Co., Ltd. (Hubei, China). Sodium chloride was acquired from Carlo Erba Reagenti (Cornaredo MI, Italy). Phosphoric acid and potassium dihydrogen orthophosphate were obtained from Fisher Scientific (Loughborough, UK). Acetone, chloroform, and methanol were of analytical and HPLC grade.

2.2. Preparation of ibuprofen-loaded SLNs (IBSLNs) and nanoemulsions (IBNEs)

IBSLNs and IBNEs were prepared by the hot high-pressure homogenization method (HPH) (Chantaburanan et al., 2017). Ibuprofen (1% *w*/w) was dissolved in 9% *w*/w melted lipid at 80 °C. The lipid was composed of CP and S378 at different ratios, *i.e.*, 1:0, 1:1, or 0:1. The hot lipid phase was dispersed in a hot aqueous solution (80 °C) containing an emulsifier (1.2% *w*/w TG450 or 2.5% w/w P188) with a homogenizer (IKA T25 Ultra-turrax®, Staufen, Germany) operated at 8000 rpm for 1 min. Then, the hot preemulsion was heated to 90 °C and homogenized with a high-pressure homogenizer (APV 2000, UK) at a pressure of 500 bar for 3 cycles. The hot mixture was cooled to ambient temperature. NEs were prepared in the same manner as SLNs, except that the lipid phase was replaced with M812. The compositions of all formulations are shown in Table 1.

Table 1
The compositions of IBSLNs and IBNEs (% *w*/w).

Formulations	% w/w						
	CP	S378	M812	Ibuprofen	TG450	P188	H_2O q.s.to
IBSLN1-TG450	9	–	–	1	1.2	–	100
IBSLN2-TG450	4.5	4.5	–	1	1.2	–	100
IBSLN3-TG450	–	9	–	1	1.2	–	100
IBNE-TG450	–	–	9	1	1.2	–	100
IBSLN1-P188	9	–	–	1	–	2.5	100
IBSLN2-P188	4.5	4.5	–	1	–	2.5	100
IBSLN3-P188	–	9	–	1	–	2.5	100
IBNE-P188	–	–	9	1	–	2.5	100

2.3. Physicochemical stabilities of ibuprofen-loaded SLN dispersions (IBSLNs) and nanoemulsions (IBNEs)

2.3.1. Particle size and size distribution

The average particle size (z-average) and polydispersity index (PDI) for all IBSLN and IBNE samples were assessed using photon correlation spectroscopy (PCS) with a Zetasizer Nano Series ZS instrument (Malvern Instruments, Malvern, UK). To obtain appropriate scattering intensities, the samples were diluted with bidistilled water prior to the measurements. These measurements were conducted at a scattering angle of 173° and a temperature of 25 °C. The particle sizes for each sample were measured in triplicate.

Owing to the measurement size range of PCS (0.3 nm to 10.0 μm), laser diffraction (LD) was employed to evaluate larger particles using a Mastersizer Hydro2000 system (Malvern Instruments, Malvern, UK). The data obtained from LD provided the volume distribution of the particles. The results are presented as the diameters for 50% (d(0.5)), 90% (d(0.9)), and 95% (d(0.95)) of the particles. The particle sizes were determined with the Mie characterization method, with the real refractive and imaginary refractive indices set at 1.456 and 0.01, respectively. The measurements were carried out in triplicate.

2.3.2. Zeta potential (ZP)

The ZP values of all formulations were evaluated with a Zetasizer Nano Series ZS instrument (Malvern Instruments, Malvern, UK). Prior to the measurement, a small portion of the sample (20 μL) was diluted in bidistilled water (10 mL) and adjusted to a conductivity of 50 μS/cm with a 0.9% *w/v* sodium chloride solution.

2.3.3. Encapsulation efficiency (E.E.)

The E.E. of ibuprofen in the IBSLNs and IBNEs was examined by the ultrafiltration method. Approximately 1 g of the IBSLNs or IBNEs was placed on the filter membrane of an ultracentrifuge tube (Amicon® Ultra-4, molecular weight cutoff 30 kDa, Massachusetts, USA) and centrifuged at 5000 rpm for 60 min using a Kubota Model 6930 (Kubota, Osaka, Japan). The free ibuprofen in the ultrafiltrate was subsequently analyzed with high-performance liquid chromatography (HPLC) (Chantaburanan et al., 2017). In summary, the HPLC system used was a Shimadzu LC10 automatic sampler (Shimadzu, Kyoto, Japan). A reversed-phase Phenomenex® Luna C18 column (4.6 × 250 mm i.d., packed with 5 μm Luna-C18) served as the stationary phase. The mobile phase consisted of methanol and water in an 80:20 (*v*/v) ratio, the pH was adjusted to 3.0 with phosphoric acid and the flow rate was 1.0 mL/min. The injection volume was 20 μL, and the UV detector was set at 227 nm. The %E.E. for the IBSLNs and IBNEs was calculated as shown in Eq. (1).

$$\%\text{E.E.} = \frac{\text{Total amount of ibuprofen} - \text{Amount of free ibuprofen}}{\text{Total amount of ibuprofen}} \times 100 \quad (1)$$

2.3.4. Differential scanning calorimetry (DSC)

The %CI was determined for all IBSLN and IBNE samples using a Mettler DSC1 instrument (Mettler Toledo, Greifensee, Switzerland). Briefly, the IBSLN dispersions (10–20 mg) or bulk lipids (1–2 mg) were weighed into a 40 μL aluminum pan and sealed with an aluminum pan lid. The sample was heated from 25 °C to 90 °C and then cooled to 25 °C with heating/cooling rates of 5 °C/min, under a nitrogen flow rate of 80 mL/min. An empty aluminum pan sealed with an aluminum pan lid served as the reference. The melting temperature (T_m), melting enthalpy (ΔH), and onset temperature (T_{onset}) were analyzed using STARe DB V 11.00 software. The %CI of the IBSLNs was calculated as indicated in Eq. (2):

$$\%\text{CI} = \frac{\Delta\text{H } \textit{SLN dispersion}}{\Delta\text{H } \textit{bulk lipid mixture} \text{ X\%lipid phase}} \times 100 \quad (2)$$

2.3.5. Wide angle X-ray diffraction

The polymorphic forms of the lipid matrix were assessed through wide angle x-ray scattering (WAXS) using a PANalytical X'Pert PRO machine, equipped with a copper anode, under room temperature conditions. To convert dispersions into a paste-like consistency, a mixture was created by combining 1.0 mL of dispersion with 0.3 g of locust bean gum powder before proceeding with the evaluation. These samples were then positioned onto a thin aluminum holder. The scans were carried out from 3° to 40° using an incremental step width of 0.02° (0.5 s per step). Finally, the d-spacing values were computed based on Bragg's equation.

2.4. Occlusive study

An *in vitro* occlusive study was performed by the de Vringer method (Wissing et al., 2001). Briefly, 50 mL beakers were filled with 30 mL of water and covered with filter paper (Whatman No. 5, Maidstone, UK). The samples were spread onto the filter paper and placed in a desiccator, where the relative humidity was maintained at approximately 75% with a saturated sodium chloride solution. The experiments were conducted at 32 °C for 48 h. The amount of water loss was determined by weighing the beakers containing water after the 48-h sample application period. Each formulation was assessed in triplicate. A beaker covered with filter paper, but without any sample, was used as a reference (no occlusive effect). The occlusive factor (F) was calculated according to Eq. (3).

$$\text{F} = \frac{(\text{A} - \text{B})}{\text{A}} \times 100 \quad (3)$$

where A is the water loss without a sample (reference) and B is the water loss with a sample.

2.5. In vitro release study

In vitro release studies for the IBSLNs and IBNEs were conducted with static Franz diffusion cells (10 mL volume, 1.5 cm diameter, Crown Scientific, Massachusetts, USA) fitted with mixed cellulose ester membranes (0.1 μm pore size). A pH 5.5 phosphate buffer served as the receptor medium. The receptor medium was maintained at 32 ± 0.5 °C and continuously stirred at 300 rpm with a magnetic stirrer. To assess and compare the ibuprofen release levels for each formulation, 300 μL of the IBSLN or IBNE dispersion was applied to the membrane on the donor side. At specified time intervals (0, 1, 2, 4, 6, 8, 10, 12, and 24 h), 500 μL of the receptor medium was collected, and an equal volume of fresh receptor medium was introduced into the receptor chamber of the Franz diffusion cell. Each formulation was tested in triplicate. The amounts of ibuprofen released were determined with HPLC.

2.6. Long-term stability

All IBSLNs and IBNEs were stored at three different temperatures (4 °C, RT, and 40 °C) for 180 days. The long-term stabilities of all formulations were determined for the particle size, size distribution, zeta potential, ibuprofen content, and % E.E.

2.7. Determination of in vitro skin permeation

2.7.1. Preparation of epidermis

Samples of human skin were obtained *via* abdominoplasty surgeries for 25 to 60-year-old female patients supported by Yanhee Hospital. The epidermal membranes were prepared by the heat separation technique (Chantasart et al., 2007; Junyaprasert et al., 2013). Briefly, human skin without subcutaneous fat and connective tissue was immersed in water at 60 °C for 2 min. The epidermis was peeled off from the underlying dermis, soaked in PBS pH 7.4, and stored at −20 °C until use. It was then soaked in PBS pH 7.4 overnight at 4 °C (in a refrigerator) and cut into

4.5 × 4.5 cm pieces before use. The experimental protocol was approved by the human ethics committee of Mahidol University, Thailand (project no. MU-DT/PY-IRB 2014/023.2306).

2.7.2. *In vitro skin permeation study*

In vitro skin permeation studies were performed with static Franz diffusion cells (Volume 10 mL, diameter 1.5 cm, Crown Scientific, Sommerville, USA), equipped with the excised human epidermis. To mimic the pH and temperature of blood circulation, PBS with a pH of 7.4 was used as a receptor medium at a controlled temperature of 37 ± 0.5 °C. To ensure the integrity of the epidermis, the electrical resistance of the epidermis was measured before and after the permeation study (Musazzi et al., 2018). Approximately 300 µL of the IBSLN or IBNE was applied onto the stratum corneum side of the epidermis. The receptor phase was withdrawn at determined time intervals and immediately replaced with an equal volume of fresh PBS pH 7.4. The amounts of permeated ibuprofen were determined by HPLC. At the end of the experiment, the human epidermis was removed and rinsed with water and methanol. The ibuprofen retained in the epidermis was extracted with chloroform: methanol (2:1 *v*/v) solution. Six replicates of the experiment were carried out for each formulation.

2.8. *Statistical analysis*

The differences in the physicochemical properties of the formulations after production and after determined interval times were evaluated with Student's *t*-test or one-way analysis of variance (one-way ANOVA). Significance was indicated with a *p*-value of 0.05.

3. Results and discussion

3.1. *Particle size and size distribution*

To evaluate the effects of the emulsifier and proportions of CP and S378 on the particle sizes and size distributions, IBSLNs were prepared with only CP, only S378, and with 1:1 *w*/w binary mixture of CP and S378 as the lipid phase, and these were stabilized with the 2 emulsifiers, TG450 and P188, as shown in Table 1. After production, the particle sizes of the IBSLN-TG450 and IBSLN-P188 samples were within the ranges 185–201 nm and 140–146 nm, respectively, with the PDI values of <0.15, as shown in Fig. 2. In comparing the particle sizes of the IBSLN-P188 and IBSLN-TG450 samples with the same compositions of the lipid phase (CP, S378, or a 1:1 mixture of CP and S378), IBSLN-P188 showed smaller particle sizes ($p < 0.05$). A similar result was also found for the IBNEs. The particle size of the IBNE-P188 sample was 141.6 nm which was smaller than that of IBNE-TG450 (187.4 nm) ($p < 0.05$). This suggested that the emulsifier had a strong influence on the particle size of the IBSLNs and IBNEs.

To study the long-term stabilities, all of the IBSLN and IBNE formulations were stored at three different temperatures (*i.e.*, 4 °C, RT, and 40 °C). The particle sizes of the stored IBSLN and IBNE formulations were almost constant or slightly increased compared to their initial values. The particle sizes of IBSLN-TG450 and IBSLN-P188 remained <210 and 180 nm, respectively, with PDI values lower than 0.2 (Fig. 2). For IBNEs, particle sizes <200 nm and PDI <0.15 were observed. In general, PDI <0.1 indicates monodisperse particles, PDI between 0.1 and 0.4 indicates moderately polydisperse particles, and PDI >0.4 indicates polydisperse particles (Takechi-Haraya et al., 2022). Therefore, it was concluded that all of the prepared IBSLNs and IBNEs were physically stable after storage under different conditions for 180 days except for IBSLN1-TG450 for which ibuprofen crystals were formed in the mixtures after production and storage at 4 °C, RT, and 40 °C for 180 days.

Due to the limitations of PCS, which can detect particle sizes <10 µm, the LD technique was used to determine the mean particle sizes of large particles or aggregate particles by evaluating d(0.5), d(0.90), and d (0.95). After production, the d(0.5) values of the IBSLNs and IBNEs stabilized with TG450 were higher than those stabilized with P188. The d(0.5) values of the IBSLNs and IBNEs stabilized with TG450 and P188 were within the ranges 0.209–0.220 µm and 0.185–0.192 µm, respectively, as shown in Fig. 3. In addition, d(0.90) and d(0.95) for both the IBSLNs and IBNEs were less than or equal to 0.381 µm and 0.430 µm, respectively. These results indicated an absence of microparticles (> 1 µm) in all formulations.

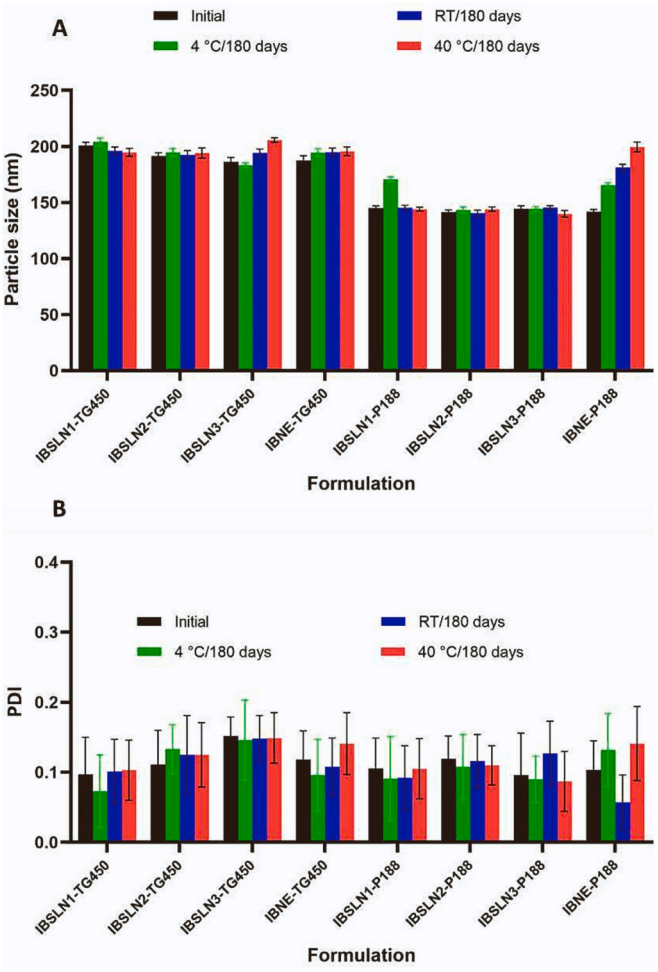

Fig. 2. Particle size (*A*) and PDI (*B*) of IBSLNs and IBNEs stabilized with TG450 and P188 after productand storage at 4 °C, RT, and 40 °C for 180 days.

After storage at different temperatures for 180 days, it was observed that the d(0.5) values of all IBSLNs and IBNEs stabilized with TG450 and P188 were comparable to their initial values. However, changes in the d (0.90) and d(0.95) values after 180 days were observed for IBSLN-TG450 (Fig. 3). In contrast, IBSLN-P188 and IBNE-P188 showed good physical stabilities after storage at room temperature for 180 days. Based on the above LD results, the long-term physical stabilities of the IBSLN and IBNE samples were achieved by using P188, which was a suitable emulsifier in this study.

Many studies have indicated the long-term physical stabilities of SLNs and NLCs, which depend on the lipid and emulsifier (Sakellari et al., 2021; Souto and Muller, 2006; Freitas and Muller, 1999; Silva et al., 2012; Wosicka-Frackowiak et al., 2015). For example, glyceride SLNs exhibited higher encapsulation efficiencies but poor stabilities. In contrast, wax SLNs showed superior physical stabilities but poor drug encapsulation. This was due to differences in crystal packing (Jenning and Gohla, 2000). Recently, *Sakellari* et al. found that SLNs prepared from Precirol® ATO showed lower physical stabilities than those prepared from Compritol® 888 ATO (Sakellari et al., 2021). The SLNs

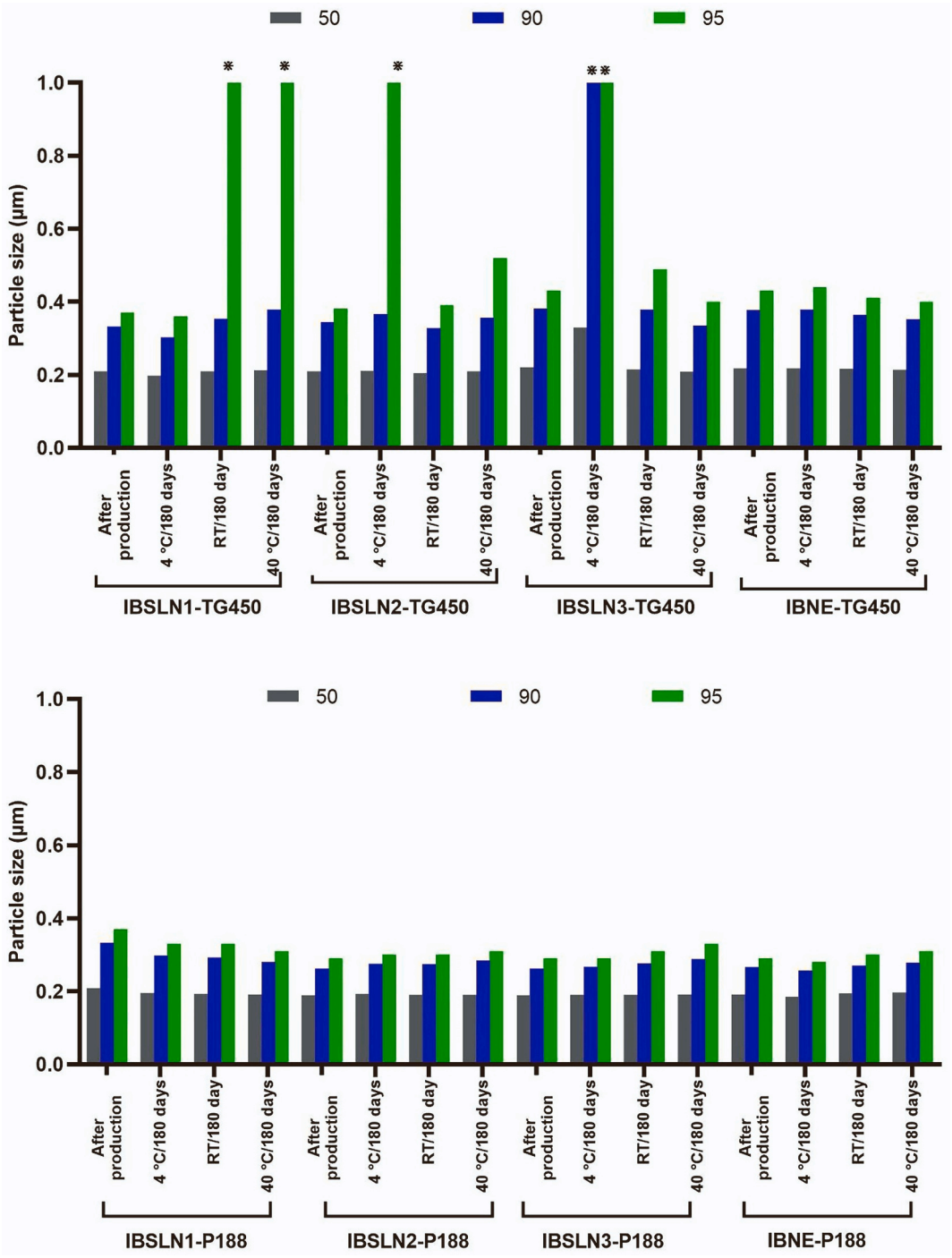

Fig. 3. Volume distribution diameter in micrometers (μm) of IBSLNs and IBNEs stabilized with TG450 (A) and P188 (B) after production and storage at 4 °C, RT, and 40 °C for 180 days. *Volume distribution diameter higher than 1 μm.

prepared from Precirol® ATO did not maintain their original sizes after 4 weeks due to the physical modifications taking place during storage. In addition to the type of solid lipid, the surfactants also played crucial roles in determining the long-term stabilities of the SLNs and NLCs. For instance, aggregation was observed for ketoconazole-loaded SLNs and NLCs stabilized with P188, while the particle sizes of those stabilized with tyloxapol remained unchanged after storage for one year at 4 °C, 25 °C, and 40 °C (Souto and Muller, 2006).

3.2. ZP values

The long-term physical stabilities of colloidal systems can be evaluated by measuring the ZP values, particularly for systems with electrostatic stabilization. In general, a ZP value higher than ±30 mV indicates good stability of the system (Kovacevic et al., 2011). Nevertheless, the use of ZP values alone may not be suitable for predicting the physical stabilities of colloidal systems containing steric stabilizers, *e.g.*, nonionic surfactants. In our study, the IBSLNs and IBNEs stabilized with TG450 (|-40 mV| - |-60 mV|) had higher ZP values than those stabilized with P188 (|-15 mV| - |-35 mV|) after storage for 180 days at 4 °C, RT, and

40 °C. The different ZP values were due to the different chemical structures of the emulsifiers. The IBSLNs and IBNEs stabilized with TG450 showed higher ZP values owing to strong interactions between water and the polyglycerol linked methylglucose molecules of TG450, which generated negatively charged hydroxyl ions at the surfaces of the particles (Kovacevic et al., 2011). Although the ZP values of the IBSLNs and IBNEs stabilized with TG450 were higher than those stabilized with P188, the IBSLNs and IBNEs stabilized with P188 showed higher physical stabilities, as mentioned above. This was due to the steric hindrance of P188 which prevented particle-particle aggregation (Lotfy et al., 2021).

3.3. DSC studies

In previous studies, the lipid matrices of some SLNs prepared by hot HPH solidified in different crystalline forms or remained in the liquid state depending on the chemical nature of the lipid and the composition of the formulation (Naseri et al., 2015; Bunjes and Koch, 2005). Since the polymorphic form of the lipid matrix has an impact on the drug entrapment efficiencies, drug release profiles, and stabilities of the SLN dispersions, DSC analyses were used to determine the lipid crystallinity after recrystallization process and to monitor the polymorphic transitions of IBSLN-TG450 and IBSLN-P188 during storage at 4 °C, RT, and 40 °C for 180 days as shown in Table 2 and Supplementary data 1. After production, peaks for ibuprofen melting were not observed for all IBSLN formulations, suggesting that the ibuprofen had completely dissolved in the lipid matrices of SLNs. In addition, all of the IBSLN formulations showed melting temperatures lower than those of the bulk lipids at the same ratio of CP and S378. This was due to the much smaller sizes of the SLNs, which led to large surface-to-volume ratios of the SLNs and less ordered structures (Kovacevic et al., 2011).

Concerning the effect of incorporation of S378 into CP-matrix stabilized with the same emulsifier, the %CI of the IBSLN2 sample was lower than that of the IBSLN1 sample regardless of the emulsifier used (Table 2). This implied that the addition of a secondary lipid (S378) into the CP disturbed the crystalline arrangement of the CP matrix. No melting endotherm was seen for IBSLN3 in the DSC chromatogram, which indicated a supercooled melt of the S378 matrix. Similar to the previous studies, supercooled melts were reported for SLNs prepared from S378 and Witepsol® E85 (Teeranachaideekul et al., 2017; Uner et al., 2005). For the IBNEs, no melting peak was observed due to the liquid states of the NEs and solubilization of ibuprofen in the M812.

Table 2
Onset temperature (T_{onset}), melting point (T_m), melting enthalpy (ΔH), and %CI of IBSLN formulations after production and storage at 4 °C, RT, and 40 °C for 180 days.

Formulation	Condition	T_{onset}(°C)	T_m (°C)	ΔH (J/g)	%CI
IBSLN1-TG450	Initial	42.62	47.32	−13.90	78.18
	4 °C/180 days	42.61	47.31	−18.74	105.40
	RT/180 days	41.98	47.09	−13.89	78.12
	40 °C/180 days	43.50	46.21	−3.66	20.59
IBSLN2-TG450	Initial	31.60	40.15	−1.09	14.91
	4 °C/180 days	37.55	43.11	−5.21	71.27
	RT/180 days	32.33	40.22	−1.25	17.10
	40 °C/180 days	29.40	38.33	−0.97	13.27
IBSLN3-TG450	Initial	–	–	0.00	0.00
	4 °C/180 days	32.39	34.50	−1.79	67.42
	RT/180 days	32.08	38.97	−1.01	38.04
	40 °C/180 days	32.58	37.23	−0.55	20.72
IBSLN1-P188	Initial	42.74	47.27	−0.24	1.35
	4 °C/180 days	32.52	45.59	−11.57	65.07
	RT/180 days	42.26	46.63	−0.83	4.67
	40 °C/180 days	43.04	46.95	−0.5	2.81
IBSLN2-P188	Initial	–	–	0	0
	4 °C/180 days	36.35	42.14	−3.85	52.66
	RT/180 days	–	–	0	0
	40 °C/180 days	–	–	0	0
IBSLN3-P188	Initial	–	–	0	0
	4 °C/180 days	32.27	36.29	−1.11	41.81
	RT/180 days	–	–	0	0
	40 °C/180 days	–	–	0	0

Concerning the effect of emulsifier on the %CI, IBSLN1-TG450 (~78%) and IBSLN2-TG450 (~15%) showed higher %CI than IBSLN1-P188 (~1.35%) and IBSLN2-P188 (~0%). The chemical structures of the emulsifiers are shown in Fig. 1. TG450 is a nonionic emulsifier comprising a hydrophobic component (distearate) and a hydrophilic component (polyglyceryl and glucose). The hydrophobic part, which contains two C-18 hydrocarbon chains, may be incorporated into the lipid cores of lipid nanoparticles during emulsification. These hydrocarbon chains could promote crystallization of the SLN lipid matrix during cooling and storage. On the other hand, P188 is a hydrophilic-hydrophobic-hydrophilic block copolymer capable of forming a U-shaped conformation at the particle interface, which in turn slows the polymorphic transition of the SLNs (Salminen et al., 2014). The poly (propylene oxide) of P188 might distort or retard the crystallization of the lipid matrix in the SLNs, as indicated by the lower %CI of IBSLN-P188 compared to IBSLN-TG450.

In a study of long-term storage, the %CI for all IBSLN formulations stored at 4 °C for 180 days was drastically increased, particularly for IBSLN-TG450. In contrast, the %CI of IBSLNs stored at 40 °C was low, indicating incomplete crystallization of the lipid matrix. These results suggested that storage temperature affected the % CI of the IBSLNs as shown in Table 2.

The above results showed that the surfactants, incorporation of a secondary lipid in the matrix, and the storage temperature could affect the crystallization of the lipid matrix, which might subsequently affect the physical and chemical stabilities, drug entrapment efficiencies, drug release properties, and dermal drug permeation rates of the IBSLNs.

3.4. WAXD analysis

WAXD was used to investigate the polymorphic behaviors of the SLNs. Fig. 4 shows the X-ray diffractograms for IBSLN-TG450, and IBSLN-P188 after production and storage at 4 °C, RT, and 40 °C for 180 days. As previously reported (Chantaburanan et al., 2017), the X-ray diffractogram for bulk CP displayed the peaks at 2 Thata of 21.31° and 23.63°, which correspond to lattic spacings of 0.42 and 0.38 nm respectively, demonstrating an orthorhombic subcell. Conversely, the bulk S378 showed β'/β_i modification with peak reflections at 2 Thata of 19.29°, 21.05°, and 24.01°. These peaks correlate with lattice spacing of 0.46, 0.42, and 0.37 nm, respectively. The ibuprofen data indicated a crystalline state with two low-intensity peaks at 6.05° and 22.21° with well-defined peaks at 16.71°, 19.28°, and 20.16°. In addition, the addition of S378 into the CP matrix did not affect the polymorphism of the CP but decreased the intensities of the peaks at 21.31° and 23.63°, indicating a less ordered structure for the CP matrix. Comparing the peak intensity of IBSLN-P188 and IBSLN-TG450 prepared with the same ratios of CP and S378, IBSLN-P188 showed lower peak intensities. Therefore, the crystallization processes of the IBSLN lipid matrices could be disturbed or retarded by the addition of S378 into the CP matrix and stabilized with P188.

3.5. Encapsulation efficiency (E.E.)

Table 3 shows the ibuprofen E.E. percentages for all of the IBSLNs and IBNEs after production. The %E.E. of ibuprofen after production for all formulations was higher than 98%, implying that ibuprofen was almost entirely entrapped in the lipid nanoparticles. No statistically significant differences were observed in E.E. for any of the formulations ($p > 0.05$).

After storage at the different temperatures for 180 days, a decreased E.E. was observed for the IBSLN samples stored at 4 °C. This was attributed to accelerate of lipid crystallization at the low temperature (4 °C), leading to ibuprofen expulsion from the SLN matrix. However,

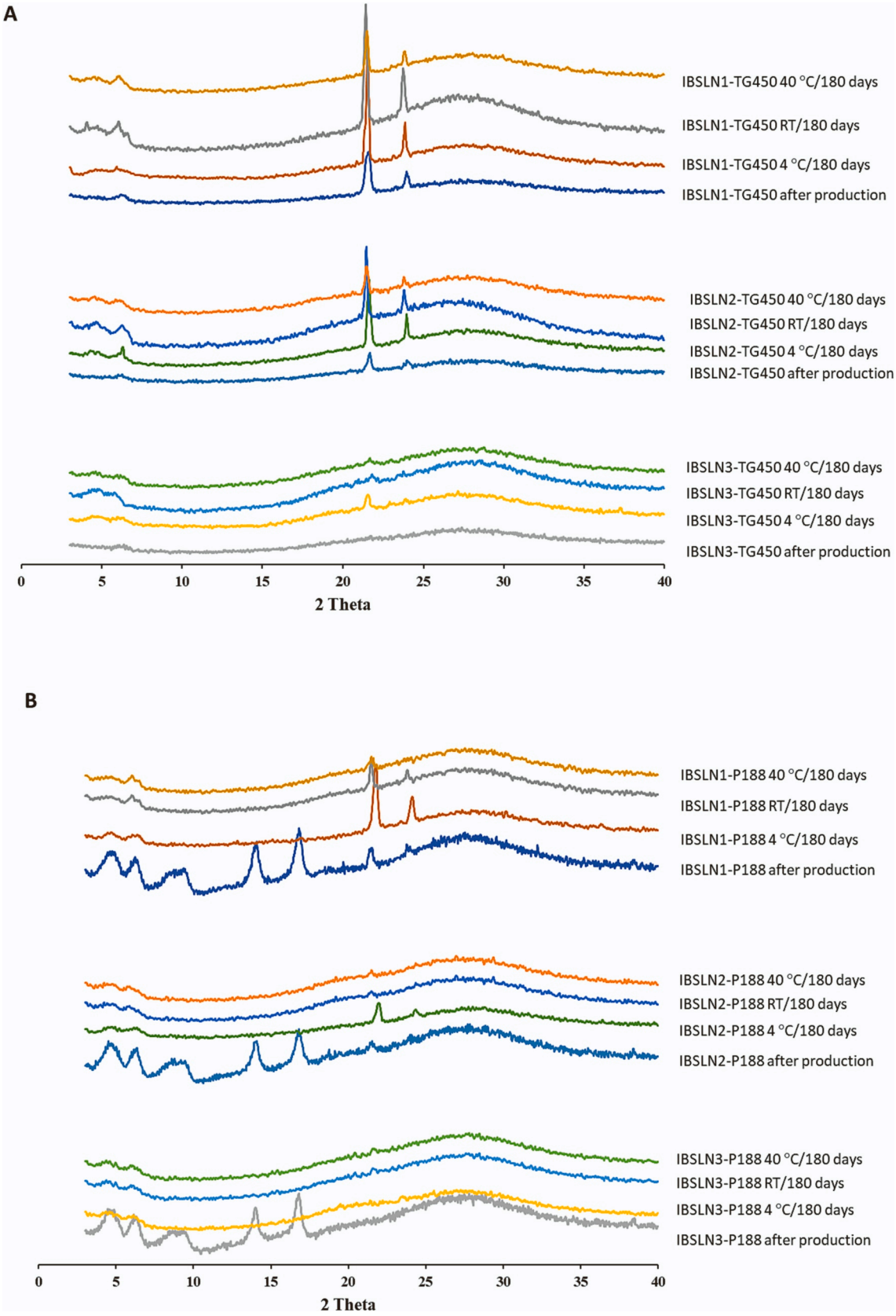

Fig. 4. X-ray diffractograms of IBSLN-TG450 formulations (A) and IBSLN-P188 formulations (B) after production and storage at 4 °C, RT, and 40 °C for 180 days.

Table 3
%E.E. of ibuprofen in IBSLNs and IBNEs stabilized with TG450 or P188 after production and storage at 4 °C, RT, and 40 °C for 180 days (mean ± SD, $n = 3$).

Formulation	Condition	% E.E.	
		TG450	P188
IBSLN1	Initial	99.69 ± 0.11	99.41 ± 0.92
	4 °C/ 180 days	40.52 ± 2.58	79.82 ± 2.33
	RT/ 180 days	98.67 ± 1.01	98.32 ± 1.98
	40 °C/ 180 days	98.01 ± 0.32	98.97 ± 1.78
IBSLN2	Initial	99.17 ± 1.12	98.86 ± 1.32
	4 °C/ 180 days	75.22 ± 1.09	89.64 ± 2.03
	RT/ 180 days	96.27 ± 3.22	98.58 ± 1.93
	40 °C/ 180 days	97.80 ± 1.42	96.78 ± 1.53
IBSLN3	Initial	98.86 ± 1.18	98.96 ± 2.01
	4 °C/ 180 days	88.52 ± 1.22	97.08 ± 2.04
	RT/ 180 days	96.45 ± 2.42	98.07 ± 1.27
	40 °C/ 180 days	95.65 ± 3.21	95.99 ± 1.19
IBNE	Initial	99.98 ± 0.98	99.23 ± 1.42
	4 °C/ 180 days	97.06 ± 1.18	98.73 ± 2.39
	RT/ 180 days	97.88 ± 0.58	95.23 ± 2.01
	40 °C/ 180 days	91.57 ± 1.32	88.97 ± 1.57

when S378 was added to the CP matrix (for IBSLN1 and IBSLN2 stabilized with the same emulsifier) or the lipid matrix was made from only S378 (IBSLN3), less ibuprofen was expelled from the IBSLN dispersions stored at 4 °C. This was explained by the formation of a less ordered structure, as indicated by the low %CI and/or melting enthalpy. In addition, IBSLN-P188 samples (IBSLN1, IBSLN2, and IBSLN3) exhibited a higher %E.E. than IBSLN-TG450 samples after storage at 4 °C for 180 days. The low %E.E. seen for ibuprofen after storage for 180 days at 4 °C was attributed to the increased %CI, as shown in Table 2, which resulted in drug expulsion from the lipid matrix of the SLNs. According to the literature, an increase in the %CI indicates the formation of an ordered structure in the lipid matrix, which results in less space for drug accommodation (Ghasemiyeh and Mohammadi-Samani, 2018; Salvi and Pawar, 2019). No differences were observed for the %E.E. of IBNE-TG450 and IBNE-P188 ($p > 0.05$) because the IBNEs were prepared from MCT, which did not crystallize during storage. Based on the above results, the optimized IBSLN was obtained by selecting suitable surfactants and ratios of the binary lipid matrix.

3.6. Occlusion factor

Due to the formation of nanosized solid-state particles, SLNs are known to exhibit higher occlusion factors than NEs after application on the skin (Wissing and Muller, 2002). Fig. 5 shows the occlusion factors for IBSLNs and IBNEs stabilized with TG450 and P188. It was found that addition of S378 into the CP matrix decreased the occlusion factor due to lower crystallinity of the lipid matrix. In a comparison of the effects of emulsifiers on the occlusion factors of IBSLNs prepared with the same lipid phase composition, it was found that IBSLN1 and IBSLN2 stabilized with TG450 exhibited higher occlusion factors than IBSLN1 and IBSLN2 stabilized with P188 ($p < 0.05$). This was attributed to the differences in lipid crystallinity as demonstrated by the DSC and XRD analyses. Although the IBSLN3 and IBNE samples stabilized with TG450 and P188 did not show melting endotherms in the DSC thermograms, IBSLN3 exhibited a higher occlusion factor than IBNE ($p < 0.05$). This finding indicated that the supercooled melt of the IBSLNs had a higher occlusion factor than the liquid state of the IBNEs.

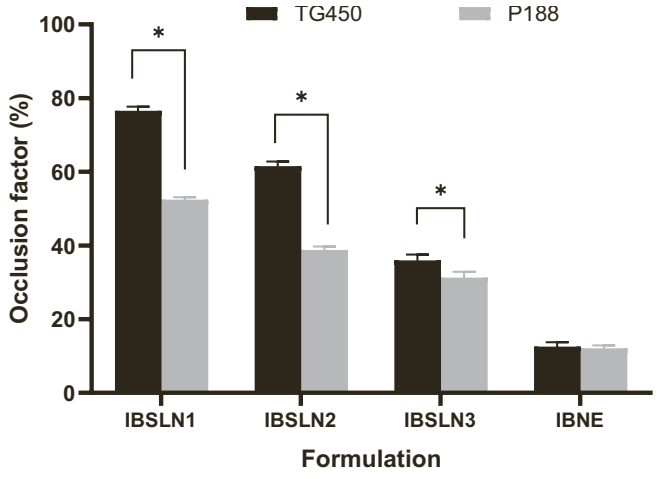

Fig. 5. Occlusion factors of IBSLNs and IBNEs stabilized with TG450 and P188 after production. * Statistically significant difference at 95% confidence interval ($p < 0.05$).

3.7. In vitro release study

The different crystallization behaviors of the IBSLN-TG450 and IBSLN-P188 samples might affect the ibuprofen release profiles of the IBSLNs. Therefore, the cumulative amounts of ibuprofen released from the IBSLN-TG450 and IBSLN-P188 samples were compared. In addition, the amounts of ibuprofen released from the IBSLN and IBNE samples after storage at RT for 180 days were measured and compared to the initial time to observe the effects of storage time on the ibuprofen release profiles for the IBSLNs and IBNEs.

In a comparison of the cumulative amounts of ibuprofen released at 24 h, IBSLN1-TG450 showed the highest ibuprofen release ($p < 0.05$), followed by IBSLN2-TG450 and IBSLN3-TG450, as illustrated in Fig. 6. This suggested that incorporation of S378 into the CP matrix retarded the release of ibuprofen from the IBSLN2-TG450 sample. In contrast, the cumulative amount of ibuprofen released from IBSLN-P188 was not significantly different ($p > 0.05$). As shown in Table 2, the %CI for all IBSLN-P188 samples was lower than 2.0%, indicating that the lipid matrix of the IBSLN-P188 formed a supercooled melt rather than a crystalline structure. As a result, no difference was observed for the cumulative amount of ibuprofen released from IBSLN-P188 ($p > 0.05$).

A comparison of the *in vitro* release profiles for IBSLNs containing different emulsifiers showed that the cumulative amounts of ibuprofen released from the IBSLN-P188 samples after 24 h tended to be higher than those for the IBSLN-TG450 samples, which contained the same lipid matrices (Fig. 6). As previously reported (Chantaburanan et al., 2017), the ibuprofen was localized within the tiny nanocompartments of S378 in the CP matrix of IBSLN2-TG450. This led to the low amount of ibuprofen released from IBSLN2-TG450. Due to the supercooled melt

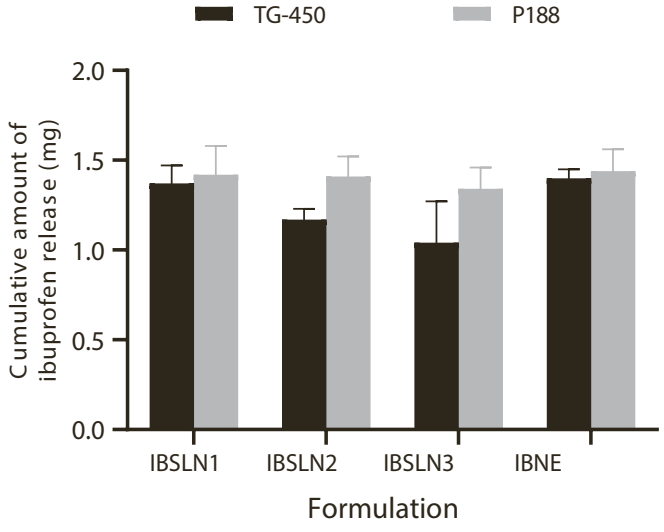

Fig. 6. Cumulative amounts of ibuprofen released (mg) from IBSLNs and IBNEs stabilized with TG450 and P188 at 24 h.

formed by IBSLN-P188 (IBSLN1-P188, IBSLN2-P188, and IBSLN3-P188), the ibuprofen was homogeneously distributed in the lipid matrix, as indicated by the DSC and XRD analyses. Therefore, the ibuprofen diffused more readily from the lipid matrix of IBSLN-P188 than from the matrix of IBSLN-TG450. These results indicated that emulsifiers had an impact on the crystallization of the lipid matrices, and formation of the inner structures of the CP matrices and subsequently affected the amounts of ibuprofen released from the IBSLNs. In the case of IBNEs, no difference was observed for the cumulative amounts of ibuprofen released from IBNE-TG450 and IBNE-P188 samples ($p > 0.05$).

To study the effects of storage time on the *in vitro* release profiles of the IBSLN and IBNE samples, the amounts of ibuprofen released from the IBSLNs and IBNEs were determined after storage at RT for 180 days and compared to the initial time amounts, as depicted in Fig. 7. After 180 days of storage, the amounts of ibuprofen released from the IBSLNs were comparable to the initial levels ($p > 0.05$), except for IBSLN1-TG450 ($p < 0.05$). Therefore, the storage time had a small effect on the amount of ibuprofen released from the IBSLNs.

3.8. In vitro skin permeation study

An *in vitro* skin permeation study was performed with PBS pH 7.4 at 37 ± 0.5 °C. The sink condition of all Franz diffusion cells was maintained during the experiments. In addition, the resistance of the epidermis was evaluated before and after the experiments to confirm the barrier properties of the epidermis during the experiment. The epidermis resistances before (17–26 kΩ/cm^2) and after (15–24 kΩ/cm^2) the experiments were almost constant, indicating the epidermal integrity (Chantasart et al., 2007; Ibrahim and Li, 2010).

The amounts of ibuprofen permeated into the receptor phase and the amounts of ibuprofen retained in the epidermis were determined after 24 h. Fig. 8 shows the cumulative amounts of ibuprofen permeated into the receptor media over 24 h from IBSLN and IBNE samples stabilized by TG450 and P188. The cumulative amount of ibuprofen permeated from the IBSLNs was significantly higher than that from the IBNEs ($p < 0.05$). In the *in vitro* release studies, the amounts of ibuprofen released from the IBNEs tended to be higher than those from the IBSLNs, as previously discussed. According to Fick's first law of diffusion, the rate for diffusion of a substance depends on the concentration gradient. The higher release rate of the IBNEs was expected to enable more ibuprofen permeation into the receptor phase. However, in this study, IBSLNs showed higher permeation into the receptor phase than the IBNEs, especially for IBSLN-TG450. The enhanced drug penetration into the skin was attributed to occlusion, *e.g.*, covering of the skin with an impermeable film or the use of formulations that provided occlusive effects (oleaginous ointments) (Hafeez and Maibach, 2013). Numerous studies have also shown that the occlusive properties of SLNs enhanced drug penetration into the deeper skin layer (Teeranachaideekul et al., 2008; Bhaskar et al., 2008; Gonullu et al., 2015; López-García and Ganem-Rondero, 2015), which led to facile permeation of the drug through the receptor phase. Therefore, the higher amounts of ibuprofen permeated in the receptor phases of the IBSLNs could have been due to the higher occlusion factors of the IBSLNs. In contrast, the IBNEs exhibited low occlusion factors. Due to the high release rates and low occlusion, the IBNEs exhibited more ibuprofen retained in the epidermis but less ibuprofen permeated into the receptor phase.

Among the IBSLN-TG450 formulations, IBSLN1-TG450 showed the highest cumulative amount of ibuprofen permeated after 24 h ($p < 0.05$), followed by IBSLN2-TG450 and IBSLN3-TG450, respectively. The highest permeation level of IBSLN1-TG450 was due to the higher release of ibuprofen and the greater occlusion factor relative to those of IBSLN2-TG450 and IBSLN3-TG450.

Although the amounts of ibuprofen released from the IBSLN-P188 formulations were comparable, the cumulative amounts of ibuprofen permeated for IBSLN1-P188 after 24 h were the highest ($p < 0.05$), while those of IBSLN2-P188 and IBSLN3-P188 were not significantly different ($p > 0.05$). The difference in ibuprofen permeation for IBSLN-P188 could be explained by the difference in occlusion.

In comparing the ibuprofen skin permeation levels of IBSLN-TG450 and IBSLN-P188 comprising the same lipid matrix compositions,

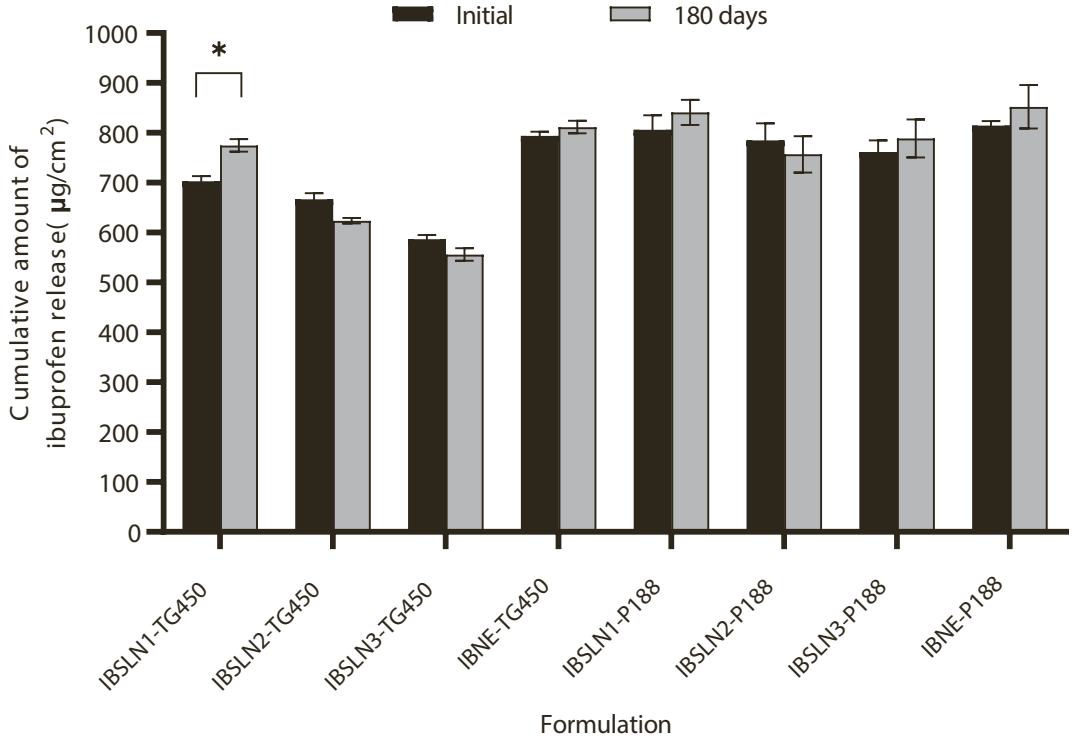

Fig. 7. Cumulative amounts of ibuprofen released from IBSLNs and IBNEs after production and storage at RT for 180 days. * Statistically significant difference at 95% confidence interval ($p < 0.05$).

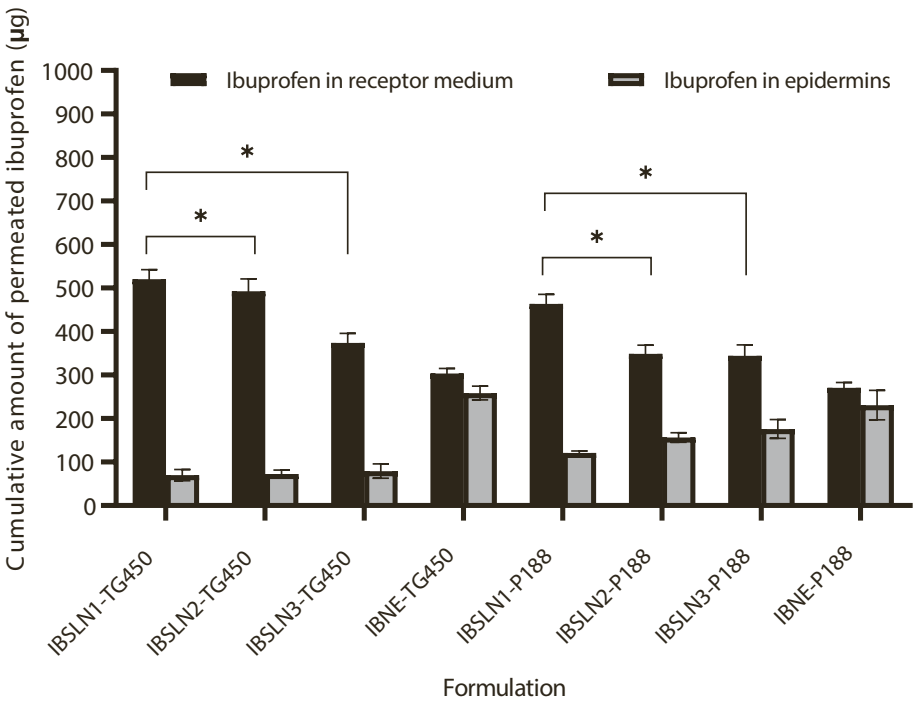

Fig. 8. Cumulative amounts of ibuprofen permeated in the receptor medium and epidermis after applying for 24 h.* Statistically significant difference at 95% confidence interval ($p < 0.05$).

IBSLN-P188 showed a lower amount of permeated ibuprofen but more retained ibuprofen, as shown in Fig. 8. This indicated that the emulsifiers had an influence on the skin permeation of ibuprofen from the IBSLNs. As previously discussed, IBSLN-TG450 had a higher %CI and occlusion factor than IBSLN-P188. These phenomena favored drug penetration into the deep skin (Souto et al., 2022; Afra et al., 2020). In comparing between IBNE-TG450 and IBNE-P188, no difference was observed in the ibuprofen permeation levels ($p > 0.05$), suggesting that the emulsifier used in this study did not promote drug penetration into the skin.

An evaluation of the effect of storage time on *in vitro* skin permeation for all formulations showed that the cumulative amounts of ibuprofen permeated after 24 h did not change or slightly increased from their initial levels, as shown in Fig. 9. These results were in accordance with those of the *in vitro* release study.

4. Conclusion

IBSLNs and IBNEs stabilized with TG450 and P188 were developed and their stabilities were observed after storage at different temperatures (4 °C, RT, and 40 °C) for 180 days. The results suggested that the long-term stability of IBSLNs was ensured by selecting a suitable

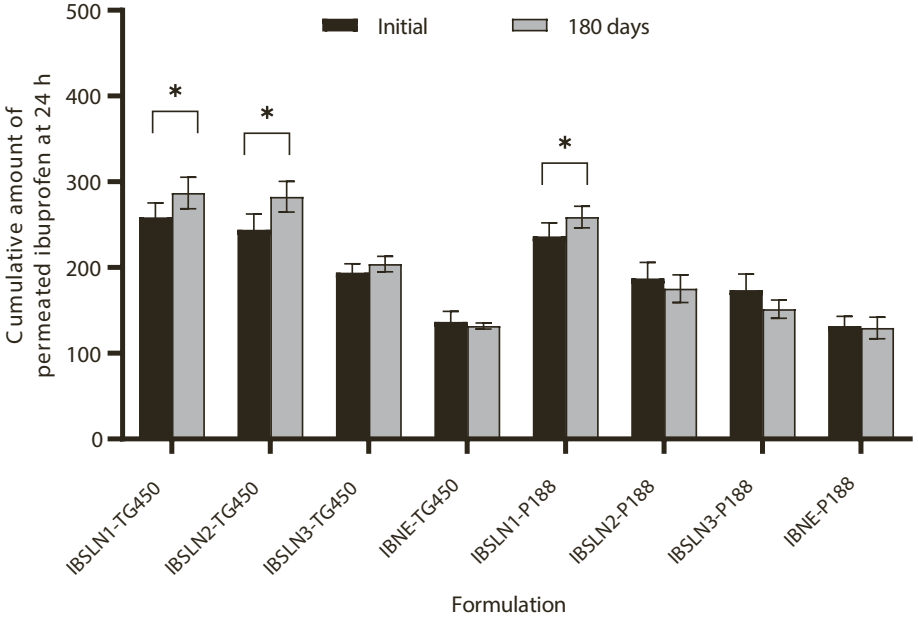

Fig. 9. Cumulative amountsof ibuprofen permeated from IBSLNs and IBNEs after production and storage at room temperature for 180 days. * Statistically significant difference at 95% confidence interval ($p < 0.05$).

emulsifier and/or incorporating S378 into the CP matrix. Changes in the *in vitro* skin performances such as the drug release profile or skin permeation rate, after storage at RT for 180 days depended on the compositions of the IBSLNs, which were related to the %CI. Therefore, the selection of suitable compositions for the lipid matrix and emulsifier, and appropriate storage conditions provided optimal formulations. In addition, changes in the %CI were useful in predicting the stabilities and performance profiles of lipid nanoparticles.

CRediT authorship contribution statement

Thitirat Chantaburanan: Conceptualization, Data curation, Formal analysis, Investigation, Methodology, Project administration, Validation, Visualization, Writing – original draft, Writing – review & editing. **Veerawat Teeranachaideekul:** Conceptualization, Data curation, Formal analysis, Methodology, Validation, Visualization, Writing – original draft, Writing – review & editing. **Anchalee Jintapattanakit:** Methodology, Writing - review & editing. **Doungdaw Chantasart:** Methodology, Writing - review & editing. **Varaporn Buraphacheep Junyaprasert:** Conceptualization, Data curation, Formal analysis, Funding acquisition, Investigation, Methodology, Project administration, Supervision, Validation, Visualization, Writing – review & editing.

Declaration of Competing Interest

The authors declare the following financial interests/personal relationships which may be considered as potential competing interests:

Varaporn Buraphacheep Junyaprasert reports that financial support was provided by Thailand Research Fund (TRF) through the Royal Golden Jubilee (RGJ) Ph.D. Program. Varaporn Buraphacheep Junyaprasert reports that DSC equipment was provided by S&J International Enterprises Public Company Limited.

Data availability

Data will be made available on request.

Acknowledgments

This research was financially supported by Thailand Research Fund (TRF) through the Royal Golden Jubilee (RGJ) Ph.D. Program (Grant No. PHD/0158/2549) and partially supported by the Thailand Research Fund and Faculty of Pharmacy, Mahidol University (IRG5780007). The DSC machine was supported by SJI Beauty and Health Science Institute, S&J International Enterprises Public Company Limited, Thailand.

Appendix A. Supplementary data

Supplementary data to this article can be found online at https://doi.org/10.1016/j.ijpx.2023.100205.

References

Afra, B., Mohammadi, M., Soleimani, M., Mahjub, R., 2020. Preparation, statistical optimization, in vitro characterization, and in vivo pharmacological evaluation of solid lipid nanoparticles encapsulating propolis flavonoids: a novel treatment for skin edema. Drug Dev. Ind. Pharm. 46 (7), 1163–1176.

Araujo, V.H.S., Delello Di Filippo, L., Duarte, J.L., Sposito, L., Camargo, B.A.F., da Silva, P.B., et al., 2021. Exploiting solid lipid nanoparticles and nanostructured lipid carriers for drug delivery against cutaneous fungal infections. Crit. Rev. Microbiol. 47 (1), 79–90.

Bhaskar, K., Krishna Mohan, C., Lingam, M., Prabhakar Reddy, V., Venkateswarlu, V., Madhusudan, Rao Y., 2008. Development of nitrendipine controlled release formulations based on SLN and NLC for topical delivery: in vitro and ex vivo characterization. Drug Dev. Ind. Pharm. 34 (7), 719–725.

Bunjes, H., Koch, M.H., 2005. Saturated phospholipids promote crystallization but slow down polymorphic transitions in triglyceride nanoparticles. J. Control. Release 107 (2), 229–243.

Bunjes, H., Westesen, K., Koch, M.H.J., 1996. Crystallization tendency and polymorphic transitions in triglyceride nanoparticles. Int. J. Pharm. 129 (1), 159–173.

Chantaburanan, T., Teeranachaideekul, V., Chantasart, D., Jintapattanakit, A., Junyaprasert, V.B., 2017. Effect of binary solid lipid matrix of wax and triglyceride on lipid crystallinity, drug-lipid interaction and drug release of ibuprofen-loaded solid lipid nanoparticles (SLN) for dermal delivery. J. Colloid Interface Sci. 504, 247–256.

Chantasart, D., Sa-Nguandeekul, P., Prakongpan, S., Li, S.K., Higuchi, W.I., 2007. Comparison of the effects of chemical permeation enhancers on the lipoidal pathways of human epidermal membrane and hairless mouse skin and the mechanism of enhancer action. J. Pharm. Sci. 96 (9), 2310–2326.

Chutoprapat, R., Kopongpanich, P., Chan, L.W., 2022. A mini-review on solid lipid nanoparticles and nanostructured lipid carriers: topical delivery of phytochemicals for the treatment of acne vulgaris. Molecules. 27 (11).

Essaghraoui, A., Belfkira, A., Hamdaoui, B., Nunes, C., Lima, S.A.C., Reis, S., 2019. Improved dermal delivery of cyclosporine a loaded in solid lipid nanoparticles. Nanomaterials (Basel). 9 (9).

Freitas, C., Muller, R.H., 1999. Correlation between long-term stability of solid lipid nanoparticles (SLN) and crystallinity of the lipid phase. Eur. J. Pharm. Biopharm. 47 (2), 125–132.

Ghasemiyeh, P., Mohammadi-Samani, S., 2018. Solid lipid nanoparticles and nanostructured lipid carriers as novel drug delivery systems: applications, advantages and disadvantages. Res. Pharm. Sci. 13 (4), 288–303.

Gonullu, U., Uner, M., Yener, G., Karaman, E.F., Aydogmus, Z., 2015. Formulation and characterization of solid lipid nanoparticles, nanostructured lipid carriers and nanoemulsion of lornoxicam for transdermal delivery. Acta Pharma. 65 (1), 1–13.

Hafeez, F., Maibach, H., 2013. Occlusion effect on in vivo percutaneous penetration of chemicals in man and monkey: partition coefficient effects. Skin Pharmacol. Physiol. 26 (2), 85–91.

Ibrahim, S.A., Li, S.K., 2010. Efficiency of fatty acids as chemical penetration enhancers: mechanisms and structure enhancement relationship. Pharm. Res. 27 (1), 115–125.

Jain, S., Patel, N., Shah, M.K., Khatri, P., Vora, N., 2017. Recent advances in Lipid-based Vesicles and Particulate Carriers for Topical and Transdermal Application. J. Pharm. Sci. 106 (2), 423–445.

Jenning, V., Gohla, S., 2000. Comparison of wax and glyceride solid lipid nanoparticles (SLN). Int. J. Pharm. 196 (2), 219–222.

Jores, K., Mehnert, W., Drechsler, M., Bunjes, H., Johann, C., Mader, K., 2004. Investigations on the structure of solid lipid nanoparticles (SLN) and oil-loaded solid lipid nanoparticles by photon correlation spectroscopy, field-flow fractionation and transmission electron microscopy. J. Control. Release 95 (2), 217–227.

Junyaprasert, V.B., Singhsa, P., Jintapattanakit, A., 2013. Influence of chemical penetration enhancers on skin permeability of ellagic acid-loaded niosomes. Asian J. Pharm. Sci. 8 (2), 110–117.

Katari, O., Jain, S., 2021. Solid lipid nanoparticles and nanostructured lipid carrier-based nanotherapeutics for the treatment of psoriasis. Exp. Opin. Drug Deliv. 18 (12), 1857–1872.

Kheradmandnia, S., Vasheghani-Farahani, E., Nosrati, M., Atyabi, F., 2010. Preparation and characterization of ketoprofen-loaded solid lipid nanoparticles made from beeswax and carnauba wax. Nanomedicine. 6 (6), 753–759.

Kovacevic, A., Savic, S., Vuleta, G., Muller, R.H., Keck, C.M., 2011. Polyhydroxy surfactants for the formulation of lipid nanoparticles (SLN and NLC): effects on size, physical stability and particle matrix structure. Int. J. Pharm. 406 (1–2), 163–172.

López-García, R., Ganem-Rondero, A., 2015. Solid lipid nanoparticles (SLN) and Nanostructured Lipid Carriers (NLC): occlusive effect and penetration enhancement ability. J. Cosmet. Dermatol. Sci. Appl. 05, 62–72.

Lotfy, N.S., Borg, T.M., Mohamed, E.A., 2021. The promising role of Chitosan-Poloxamer 188 nanocrystals in improving diosmin dissolution and therapeutic efficacy against ferrous sulfate-induced hepatic injury in rats. Pharmaceutics. 13 (12).

Lucia, M., 2017. Lipid-based nanoparticles as carriers for dermal delivery of antioxidants. Curr. Drug Metab. 18 (5), 469–480.

Musazzi, U.M., Casiraghi, A., Franze, S., Cilurzo, F., Minghetti, P., 2018. Data on the determination of human epidermis integrity in skin permeation experiments by electrical resistance. Data Brief. 21, 1258–1262.

Naseri, N., Valizadeh, H., Zakeri-Milani, P., 2015. Solid lipid nanoparticles and nanostructured lipid carriers: structure. Preparation and Application. Adv. Pharm. Bull. 5 (3), 305–313.

Pornputtapitak, W., Pantakitcharoenkul, J., Teeranachaideekul, V., Sinthiptharakoon, K., Sapcharoenkun, C., Meemuk, B., 2019. Effect of oil content on physiochemical characteristics of gamma-oryzanol-loaded nanostructured lipid carriers. J. Oleo Sci. 68 (8), 699–707.

Rawat, M.K., Jain, A., Singh, S., 2011. Studies on binary lipid matrix based solid lipid nanoparticles of repaglinide: in vitro and in vivo evaluation. J. Pharm. Sci. 100 (6), 2366–2378.

Sakellari, G.I., Zafeiri, I., Batchelor, H., Spyropoulos, F., 2021. Formulation design, production and characterisation of solid lipid nanoparticles (SLN) and nanostructured lipid carriers (NLC) for the encapsulation of a model hydrophobic active. Food Hydrocoll. Health 1. None.

Salminen, H., Helgason, T., Aulbach, S., Kristinsson, B., Kristbergsson, K., Weiss, J., 2014. Influence of co-surfactants on crystallization and stability of solid lipid nanoparticles. J. Colloid Interface Sci. 426, 256–263.

Salvi, V.R., Pawar, P., 2019. Nanostructured lipid carriers (NLC) system: a novel drug targeting carrier. Int. J. Pharm. 51, 255–267.

Shahraeini, S.S., Akbari, J., Saeedi, M., Morteza-Semnani, K., Abootorabi, S., Dehghanpoor, M., et al., 2020. Atorvastatin solid lipid nanoparticles as a promising approach for dermal delivery and an anti-inflammatory agent. AAPS PharmSciTech 21 (7), 263.

Silva, A.C., Kumar, A., Wild, W., Ferreira, D., Santos, D., Forbes, B., 2012. Long-term stability, biocompatibility and oral delivery potential of risperidone-loaded solid lipid nanoparticles. Int. J. Pharm. 436 (1–2), 798–805.
Souto, E.B., Muller, R.H., 2006. The use of SLN and NLC as topical particulate carriers for imidazole antifungal agents. Pharmazie. 61 (5), 431–437.
Souto, E.B., Baldim, I., Oliveira, W.P., Rao, R., Yadav, N., Gama, F.M., et al., 2020. SLN and NLC for topical, dermal, and transdermal drug delivery. Exp. Opin. Drug Deliv. 17 (3), 357–377.
Souto, E.B., Fangueiro, J.F., Fernandes, A.R., Cano, A., Sanchez-Lopez, E., Garcia, M.L., et al., 2022. Physicochemical and biopharmaceutical aspects influencing skin permeation and role of SLN and NLC for skin drug delivery. Heliyon. 8 (2), e08938.
Takechi-Haraya, Y., Ohgita, T., Demizu, Y., Saito, H., Izutsu, K.I., Sakai-Kato, K., 2022. Current status and challenges of analytical methods for evaluation of size and surface modification of nanoparticle-based drug formulations. AAPS PharmSciTech 23 (5), 150.
Teeranachaideekul, V., Boonme, P., Souto, E.B., Muller, R.H., Junyaprasert, V.B., 2008. Influence of oil content on physicochemical properties and skin distribution of Nile red-loaded NLC. J. Control. Release 128 (2), 134–141.
Teeranachaideekul, V., Chantaburanan, T., Junyaprasert, V.B., 2017. Influence of state and crystallinity of lipid matrix on physicochemical properties and permeation of capsaicin-loaded lipid nanoparticles for topical delivery. J. Drug Deliv. Sci. Technol. 39, 300–307.
Uner, M., Wissing, S.A., Yener, G., Muller, R.H., 2005. Solid lipid nanoparticles (SLN) and nanostructured lipid carriers (NLC) for application of ascorbyl palmitate. Pharmazie. 60 (8), 577–582.
Wissing, S., Muller, R., 2002. The influence of the crystallinity of lipid nanoparticles on their occlusive properties. Int. J. Pharm. 242 (1–2), 377–379.
Wissing, S., Lippacher, A., Muller, R., 2001. Investigations on the occlusive properties of solid lipid nanoparticles (SLN). J. Cosmet. Sci. 52 (5), 313–324.
Wosicka-Frackowiak, H., Cal, K., Stefanowska, J., Glowka, E., Nowacka, M., Struck-Lewicka, W., et al., 2015. Roxithromycin-loaded lipid nanoparticles for follicular targeting. Int. J. Pharm. 495 (2), 807–815.
Zafeiri, I., Smith, P., Norton, I.T., Spyropoulos, F., 2017. Fabrication, characterisation and stability of oil-in-water emulsions stabilised by solid lipid particles: the role of particle characteristics and emulsion microstructure upon Pickering functionality. Food Funct. 8 (7), 2583–2591.